In-line and cascaded DWDM transmission using a 15dB net-gain polarization-insensitive fiber optical parametric amplifier

M. F. C. STEPHENS,* M. TAN, V. GORDIENKO, P. HARPER, AND N. J. DORAN

Aston Institute of Photonic Technologies, Aston University, Aston Triangle, Birmingham, U.K., B4 7ET
**m.stephens@aston.ac.uk*

Abstract: We demonstrate and characterize polarization-division multiplexed (PDM) DWDM data transmission for the first time in a range of systems incorporating a net-gain polarization-insensitive fiber optical parametric amplifier (PI-FOPA) for loss compensation. The PI-FOPA comprises a modified diversity-loop architecture to achieve 15dB net-gain, and up to 2.3THz (~18nm) bandwidth. Three representative systems are characterized using a 100Gb/s PDM-QPSK signal in conjunction with emulated DWDM neighbouring channels: (a) a 4x75km in-line fiber transmission system incorporating multiple EDFAs and a single PI-FOPA (b) N cascaded PI-FOPA amplification stages in an unlevelled Nx25km recirculating loop arrangement, with no EDFAs used within the loop signal path, and (c) M cascaded PI-FOPA amplification stages as part of an Mx75.6km gain-flattened recirculating loop system with the FOPA compensating for the transmission fiber loss, and EDFA compensation for loop switching and levelling loss. For the 4x75km in-line system (a), we transmit 45x50GHz-spaced signals ('equivalent' data-rate of 4.5Tb/s) with average OSNR penalty of 1.3dB over the band at 10^{-3} BER. For the unlevelled 'FOPA-only' 25.2km cascaded system (b), we report a maximum of eight recirculations for all 10x100GHz-spaced signals, and five recirculations for 20x50GHz-spaced signals. For the 75.6km levelled system (c), we achieve eight recirculations for all 20x50GHz signals resulting in a total transmission distance of 604.8km.

OCIS codes: (060.2320) Fiber optics amplifiers and oscillators; (060.2330) Fiber optics communications; (190.4410) Nonlinear optics, parametric processes.

References and links

1. M. Islam, "Raman amplifiers for telecommunications," IEEE J. Sel. Topics Quantum Electron. **8**(3), 548-559 (2002).
2. C. Headley and G. P. Agrawal, *Raman amplification in fiber optical communication systems* (Academic, 2005).
3. R. Kashyap, "The fiber fuse - from a curious effect to a critical issue: A 25th year retrospective," Opt. express **21**(5), 6422-6441 (2013).
4. M. J. O' Mahony, "Semiconductor laser optical amplifiers for use in future fiber systems," IEEE J. Lightw. Technol. **6**(4), 531-544 (1988).
5. M. F. C. Stephens, D. Nesset, R. V. Penty, I. H. White, and M. J. Fice, "Wavelength conversion at 40 Gbit/s via four wave mixing in semiconductor optical amplifier with integrated pump laser," Electronics Letters **35**(5), 420-421, (1999).
6. Z. Li, A. M. Heidt, J. M. O. Daniel, Y. Jung, S. U. Alam, and D. J. Richardson, "Thulium-doped fiber amplifier for optical communications at 2 μm," Opt. Express **21**(8), 9289-9297 (2013).
7. N. Simakov, Z. Li, Y. Jung, J. M. O. Daniel, P. Barua, P. C. Shardlow, S. Liang, J. K. Sahu, A. Hemming, W. A. Clarkson, S. U. Alam, and D. J. Richardson, "High gain holmium-doped fibre amplifier," Opt. Express **24**(13), 13946-13956 (2016).
8. F. Poletti, N. V. Wheeler, M. N. Petrovich, N. K. Baddela, E. Numkam Fokoua, J. R. Hayes, D. R. Gray, Z. Li, R. Slavik, and D. J. Richardson, "Towards high-capacity fibre-optic communications at the speed of light in vacuum," Nat. Photonics **7**(4), 279–284 (2013).
9. V. Gordienko, M. F. C. Stephens, A. E. El-Taher, and N. J. Doran, "Ultra-flat wideband single-pump Raman-enhanced parametric amplification," Opt. Express **25**(5), 4810–4818 (2017).
10. Z. Tong, C. Lundstrom, P. A. Andrekson, M. Karlsson, and A. Bogris, "Ultralow noise, broadband phase-sensitive optical amplifiers, and their applications," IEEE IEEE J. Sel. Topics Quantum Electron., **18**(2), 1016-1032 (2012).

11. M. F. C. Stephens, M. Tan, I.D. Phillips, S. Sygletos, P. Harper, and N.J. Doran, "1.14 Tb/s DP-QPSK WDM polarization-diverse optical phase conjugation," Opt. Express **22**(10), 11840-11848 (2014).
12. A. D Ellis, M. Tan, M. A. Iqbal, M. A. Z. Al-Khateeb, V. Gordienko, G. S. Mondaca, S. Fabbri, M. F. C. Stephens, M. E. McCarthy, A. Perentos, I. D. Phillips, D. Lavery, G. Liga, R. Maher, P. Harper, N. Doran, S. K. Turitsyn, S. Sygletos, and P. Bayvel, "4 Tb/s transmission reach enhancement using 10× 400 Gb/s super-channels and polarization insensitive dual band optical phase conjugation," IEEE J. Lightw. Technol. **34**(8), 1717-1723 (2016).
13. S. Takasaka, and R. Sugizaki, "Polarization Insensitive Fiber Optical Parametric Amplifier Using a SBS Suppressed Diversity Loop," in *Optical Fiber Communication Conference* (Optical Society of America, 2016) paper M3D.4.
14. M. F. C. Stephens, V. Gordienko, and N.J. Doran, "20 dB net-gain polarization-insensitive fiber optical parametric amplifier with> 2 THz bandwidth," Opt. Express **25**(9), 10597-10609 (2017).
15. L. Grüner-Nielsen, D. Jakobsen, S. Herstrøm, B. Pálsdóttir, S. Dasgupta, D. Richardson, C. Lundström, S. Olsson, and P. Andrekson, "Brillouin Suppressed Highly Nonlinear Fibers," in *European Conference on Optical Communication* (ECOC 2012), paper We.1.F.1.
16. M. F. C. Stephens, I. D. Phillips, P. Rosa, P. Harper, and N. J. Doran, "Improved WDM performance of a fiber optical parametric amplifier using Raman-assisted pumping," Opt. Express **23**(2), 902-911 (2015).
17. A. Redyuk, M. F. C. Stephens, and N. J. Doran, "Suppression of WDM four-wave mixing crosstalk in fibre optic parametric amplifier using Raman-assisted pumping," Opt. Express **23**(21), 27240-27249 (2015).
18. J. D. Marconi, M. C. Fugihara, F. A. Callegari, and H. L. Fragnito, "In-line one-pump parametric amplifier with independent polarization gain: a field-trial demonstration," Microwave and Optical Tech. Lett. 55(**5**), 1104-1107 (2013).
19. Z. Lali-Dastjerdi, O. Ozolins, Y. An, V. Cristofori, F. Da Ros, N. Kang, H. Hu, H. C. H. Mulvad, K. Rottwitt, M. Galili, and C. Peucheret, "Demonstration of cascaded in-line single-pump fiber optical parametric amplifiers in recirculating loop transmission," in *European Conference on Optical Communication* (ECOC 2012), paper Mo.2.C.5.
20. N. El Dahdah, D. S. Govan, M. Jamshidifar, N. J. Doran, and M. E. Marhic, "Fiber Optical Parametric Amplifier Performance in a 1-Tb/s DWDM Communication System" IEEE IEEE J. Sel. Topics Quantum Electron. **18**(2), 950-957 (2012).
21. D. Elson, G. Saavedra, K. Shi, D. Semrau, L. Galdino, R. Killey, B. Thomsen, and P. Bayvel, "Investigation of bandwidth loading in optical fibre transmission using amplified spontaneous emission noise," Opt. Express **25**(16), 19529-19537 (2017).
22. M. McCarthy, N. Mac-Suibhne, S. T. Le, P. Harper, and A. D. Ellis, "High spectral efficiency transmission emulation for non-linear transmission performance estimation for high order modulation formats," in *European Conference on Optical Communication* (ECOC 2014), paper P.5.7.
23. J. Hansryd, P. A. Andrekson, M. Westlund, J. Li, and P. O. Hedekvist, "Fiber-based optical parametric amplifiers and their applications," IEEE J. Sel. Top. Quantum Electron. **8**(3), 506–520 (2002).
24. M. F. C. Stephens, A. Redyuk, S, Sygletos, I. D. Phillips, P. Harper, K. J. Blow, and N. J. Doran, "The Impact of Pump Phase-Modulation and Filtering on WDM Signals in a Fiber Optical Parametric Amplifier," in *Optical Fiber Communication Conference* (Optical Society of America, 2016), paper W2A.43.
25. J. M. Chavez Boggio, A. Guimarães, F. A. Callegari, J. D. Marconi, and H. L. Fragnito, "Q penalties due to pump phase modulation and pump RIN in fiber optic parametric amplifiers with non-uniform dispersion," Opt. Commun. **249**(4), 451-472 (2005).
26. A. Mussot, A. Durécu-Legrand, E. Lantz, C. Simonneau, D. Bayart, H. Maillotte, and T. Sylvestre, "Impact of pump phase modulation on the gain of fiber optical parametric amplifier," IEEE Photon. Technol. Lett. **16**(5), 1289-1291 (2004).
27. J. M. Chavez Boggio, J. D. Marconi, and H. L. Fragnito, "Experimental and numerical investigation of the SBS-threshold increase in an optical fiber by applying strain distributions," J. Lightw. Technol. **23**(11), 3808-3814 (2005).
28. Z. Lali-Dastjerdi, T. Lund-Hansen, N. Kang, K. Rottwitt, M. Galili, and C. Peucheret, "High-frequency RIN transfer in fiber optic parametric amplifiers," in *Conference on Lasers and Electro-Optics Europe* (CLEO-Europe 2011), paper CI2.5.
29. F. Zhang, Y. Luo, Y.Wang, L. Li, L. Zhu, Z. Chen, and C. Wu, "Experimental Comparison of Different BER Estimation Methods for Coherent Optical QPSK Transmission Systems," IEEE Photon. Technol. Lett. **23**(18), 1343-1345 (2011).

1. Introduction

Since its development in the early 1980s, the erbium doped fiber amplifier (EDFA) has reigned supreme as the *de facto* amplifier for real-world optical communication systems. In order for it to be superseded, we believe a competing technology must show not-only close equivalence for key amplifier features such as noise figure, gain bandwidth, physical size, cost etc., but also crucially offer a paradigm-shift improvement in one or more of them. So far, this set of

requirements has proven impossible to fulfil for any alternative amplifier which can span the low-loss 1550nm window of standard single mode fiber (SSMF). For example, it could be argued that distributed Raman amplification (DRA) provides such a paradigm-shift by virtue of much lower effective noise figure than lumped EDFA gain, together with a tunable gain window and wide bandwidth [1]. However, commercial take-up of Raman has been small in multi-span systems, most likely due to the high number of interacting pumps required for wide bandwidth (practicality and control issues) as well as double Rayleigh backscatter impacting performance [2]. Moreover, using the transmission fiber as gain medium, often with unknown losses situated between the fiber and the Raman pump itself (the optical distribution frame) raises pump-power margin issues, as well as potential safety concerns [3].

In the late 1980s, the development of semiconductor optical amplifiers offered significant reductions in size and power consumption compared with the EDFA, but suffered higher noise figures and data-patterning crosstalk in WDM applications [4]. They are now more typically used in single channel applications, for example as nonlinear elements [5], or commercially as gain blocks in transceivers. More recently, research in fiber amplifiers has explored dopants other than erbium, such as thulium [6] and holmium [7]. Excellent performance has been shown with very wide gain bandwidths (>100nm). However, the gain is in fixed regions of the spectrum where the transmission loss of SSMF can be high. These amplifiers will undoubtedly be employed successfully if research into micro-structured fiber reaches its potential [8].

As a competing technology, the Fiber Optical Parametric Amplifier (FOPA) certainly has potential to deliver superior performance to the EDFA on several fronts. For example, recent FOPA demonstrations have highlighted >100nm gain bandwidth between 1555-1665nm using a single pump [9], phase sensitive operation with noise figure below the 3dB quantum limit [10], and the use of phase-conjugated idlers produced via the gain process for transmission nonlinearity compensation [11,12]. However, in some ways researchers have tended to highlight eye-catching FOPA results whilst struggling to accomplish some basic yet fundamental requirements. For example, polarization insensitive operation with substantial net-gain (the topic of this work) has historically proven extremely difficult to achieve, but a recent breakthrough using a modified diversity-loop approach has highlighted a path forward [13,14]. Other FOPA issues remain persistent however. For example, the impact of pump stimulated Brillouin scattering (SBS) and its mitigation on amplified signal quality must be addressed, most likely via highly nonlinear fiber (HNLF) development [15]. Similarly, for DWDM amplification, signal-signal four wave mixing is likely to provide a limit on maximum data throughput. Promising research using Raman-assisted pumping within the FOPA aims to reduce this crosstalk [16,17]. These developments will not only unleash the full potential of the FOPA, but also progress other research employing fiber nonlinearity.

To the best of our knowledge, a net-gain polarization insensitive PI-FOPA has so far not been demonstrated within any transmission system. The closest examples include a field-trial whereby a PI-FOPA with net-*loss* was located between two fiber spans of 11km and 22km, whilst transmitting 5x10Gb/s on-off keyed signals [18]. However, due to the OSNR degradation from the FOPA loss, as well as other added noise, overall system performance would have been improved by bypassing this FOPA completely. In another paper, multiple FOPA amplifications were performed for a single 40Gb/s DPSK signal transmitted within a recirculating loop containing 80km of SSMF [19]. This is the only previous demonstration of cascaded in-line FOPA amplification, but it was a non-PI architecture, and thus the pump and signal required manual polarization alignment and this would not be scalable to DWDM operation. Importantly, the recirculating loop contained not only the FOPA in the signal path to combat loss, but also a 28dB EDFA. This makes it difficult *post hoc* to gauge the relative performance of the FOPA with respect to the EDFA. In terms of FOPA results demonstrating DWDM amplification, 26 x 100GHz-spaced 43.7Gb/s DWDM channels were amplified in a *non*-PI FOPA acting as a pre-amplifier in a transmitter terminal before a subsequent standard EDFA chain [20]. Each signal was independently manually polarization-aligned with the pump at the

terminal, which obviously prohibited in-line and/or cascaded amplification. The above achievements illustrate the importance of developing a net-gain PI-FOPA capable of amplifying multiple randomly-polarized DWDM signals within a transmission system.

In this paper, we incorporate a net-gain PI-FOPA for the first time within both an in-line transmission system and a recirculating transmission loop carrying polarization-multiplexed DWDM traffic. We explore a range of channel counts with either 100GHz or 50GHz spacing, and investigate the impact of the PI-FOPA on signal quality via BER and Q^2 measurements. Within the in-line system, we transmit a maximum of 45x50GHz-spaced signals occupying a bandwidth of 2.3THz (18.3nm). Within the recirculating loop arrangement, we achieve a maximum transmission distance of 604.8km (8 recirculations) for 20x50GHz spaced signals. We believe this to be a significant step towards a practically realized FOPA for optical communications.

2. 4 x 75km in-line transmission system incorporating black-box PI-FOPA

2.1 Experimental setup

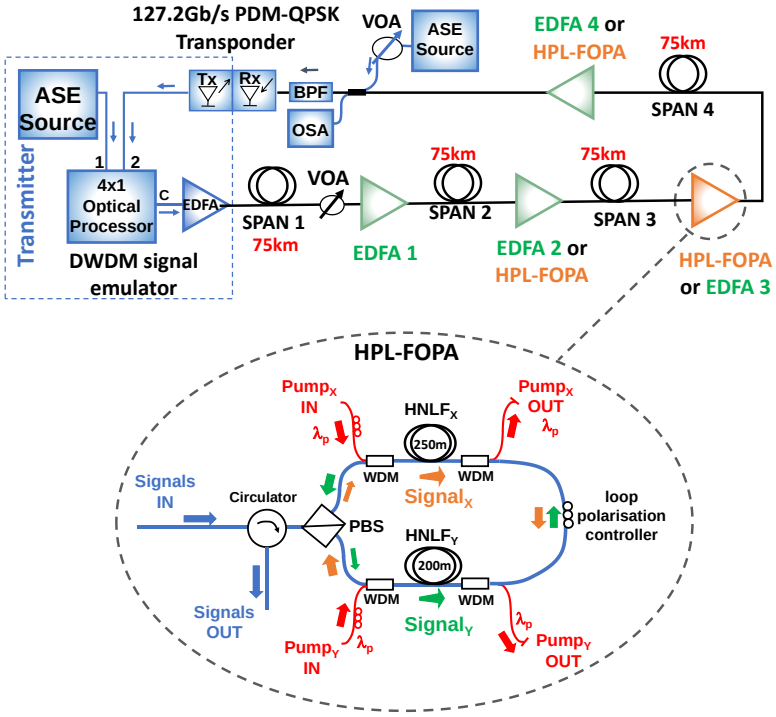

Fig. 1. Schematic of 4x75km testbed incorporating the HPL-FOPA after span 3 in example sequence EEFE. PBS=polarization beam splitter, HNLF=highly nonlinear fiber; WDM=pump add/drop filter; BPF=bandpass filter

The experimental arrangement of the in-line transmission testbed and an overview schematic of the PI-FOPA are displayed in Fig. 1. The PI-FOPA used a half-pass loop (HPL) architecture with full details of constituent parts and operation given in reference [14]. The optical transmitter (Tx) of the testbed was a commercial (Oclaro) polarization-division multiplexed (PDM) QPSK transponder with line-rate of 127.156Gb/s, including ~20% overhead for forward error correction (FEC). The payload data-rate of the transponder was 100Gb/s, delivered within a 2^{31}-1 PRBS pattern. The transponder incorporated a coherent receiver (Rx) and on-board digital signal processing (DSP) allowing real-time BER monitoring via a serial interface port. Both the Tx and Rx of the transponder were fully C-band tunable on the 50GHz ITU grid, with both set to the same carrier frequency f_{tsp} in a loop-back operating mode. To provide

neighboring DWDM channels, an optical processor (Finisar Waveshaper) was used to combine the Tx data at f_{tsp} with broadband amplified spontaneous emission (ASE). The Waveshaper was programmed to shape the ASE into multiple emulated copies of the transponder spectrum to 1GHz resolution, providing either 22x100GHz-spaced or 44x50GHz-spaced neighboring channels. In addition, the Waveshaper was used to both level the spectrum and block the ASE at frequency f_{tsp} in a 100GHz or 50GHz window depending on the signal spacing employed. In this way, no ASE was added to the transponder signal itself at the transmitter. A set of Waveshaper spectral profiles were subsequently generated, allowing f_{tsp} to be fully tuned on a 50GHz grid between 193.4THz (1550.12nm) and 195.6THz (1532.68nm), which was consistent with the FOPA gain bandwidth [14]. An additional set of Waveshaper shapes was also generated for each f_{tsp} with the ASE blocked at ±200GHz spacing from f_{tsp} in order to allow interpolation of the system noise floor at f_{tsp} for received OSNR measurements, whilst retaining the nearest neighbors to the transponder. The full DWDM multiplex was amplified via an EDFA to +1dBm per channel (i.e. a total power of 14.6dBm for 100GHz spacing or 17.6dBm for 50GHz spacing) before transmission. The use of shaped ASE to emulate neighboring channels in non dispersion compensated systems has been previously reported and shown to provide good agreement compared with real signals [21,22]. It provides a stable DWDM transmitter, allowing rapid reconfiguration without employing large amounts of equipment.

The in-line transmission system consisted of 4x75km spans of Sterlite OHLITE SSMF with the first span (span 1) incorporating a variable optical attenuator (VOA) to allow adjustment of the span-loss. As a baseline reference configuration, each span was post-amplified using a commercial variable gain (nominally 15-25dB) dual-stage gain-flattened EDFA X, where X=1-4 corresponds to the preceding span number being compensated for. Each EDFA mid-stage loss was set at 10dB and the noise figure for each EDFA was ~6dB at 25dB gain, rising to ~11dB at 15dB gain. The span 1 loss was then raised to decrease the system OSNR and generate a reference level of bit errors at the Rx (pre-FEC BER of ~10^{-6}). At this point, the amplifier-to-amplifier span losses were measured as: span1 = 26.1dB; span 2 = 15.7dB; span 3 = 15.5dB; span 4 = 16.4dB. After the final amplifier, ASE was optionally coupled with the signals via a VOA to allow OSNR adjustment at the receiver without altering any transmission span losses between measurements. The signal under test was bandpass filtered (BPF) before the Rx. The BASELINE system performance was then measured in two ways as f_{tsp} was tuned across the band: a) as a straight BER measurement with no added Rx ASE; b) by measuring the OSNR with Rx ASE to achieve 10^{-3} BER. OSNR was calculated as the ratio of signal in 0.5nm (60GHz) resolution bandwidth (RBW) to the interpolated noise power in 0.1nm (12.5GHz) RBW. Under the same span loss conditions, EDFA 2, 3 and 4 were then each replaced with the HPL-FOPA. The HPL-FOPA did not incorporate a gain flattening filter and thus had a typically curved gain spectrum [23], with ~16dB net-gain (averaged over the signal band). The gain spectrum bandwidth was ~18nm with ~5dB gain variation from maximum to minimum gain. Signal input power was dependent on the preceding span loss, but typically close to -15dBm per signal. The HPL-FOPA was operated with fixed pump powers of 35.2dBm and 34.2dBm at 1564.4nm into 250m and 200m HNLF lengths for the X and Y paths respectively (see Fig. 1). The pumps were phase modulated with three RF tones (100MHz, 320MHz and 980MHz) to mitigate SBS [14]. In operation, the pump and loop polarization controllers (PCs) of the HPL-FOPA were periodically adjusted to maintain the gain in each direction about the loop in a fixed ratio. This was performed approximately every ten minutes once the HPL-FOPA had stabilized, and would make for an easily automated control system. The signal polarization was not adjusted in any way. It should also be noted that the idlers generated within the HPL-FOPA were not specifically filtered out, but were naturally blocked at subsequent EDFAs (via out-of-band absorption), and/or at the receiver BPF.

2.2. In-line transmission system results

The received DWDM spectra under both 50GHz and 100GHz channel spacing conditions, and with no receiver ASE added are shown in Fig. 2. As shorthand, the sequence of four amplifiers under test will subsequently be referred to as $XXXX_Y$ where X=E or F for EDFA (E) or FOPA (F) respectively, and Y=50 or 100 for 50GHz or 100GHz channel spacing.

Figure 2(a) illustrates that the maximum-minimum signal peak power variation for the all-EDFA system ($EEEE_{100}$) is ~3.5dB but increases to ~6dB when the FOPA is introduced for the three configurations $EFEE_{100}$, $EEFE_{100}$ and $EEEF_{100}$. This is due to FOPA gain roll-off which is seen for wavelengths >1545nm and <1534nm, and arises from phase mismatch which is typical FOPA behavior [14,23]. For $EEEF_{100}$ (i.e. with the FOPA acting as a pre-amplifier for the receiver), the OSNR can be seen to be very similar to $EEEE_{100}$ across the band. However, with the FOPA placed earlier in the system ($EFEE_{100}$ and $EEFE_{100}$), OSNR is reduced at the spectral extremes due to the gain roll-off reducing signal power. Figure 2(b) shows that doubling the spectral efficiency by using 50GHz-spaced signals maintains both the overall spectral shape and signal power levels but, by close inspection of wavelength range 1531-32nm, the noise floor can be seen to increase by ~1.5dB. This is probably due to increased crosstalk from signal-signal four-wave mixing.

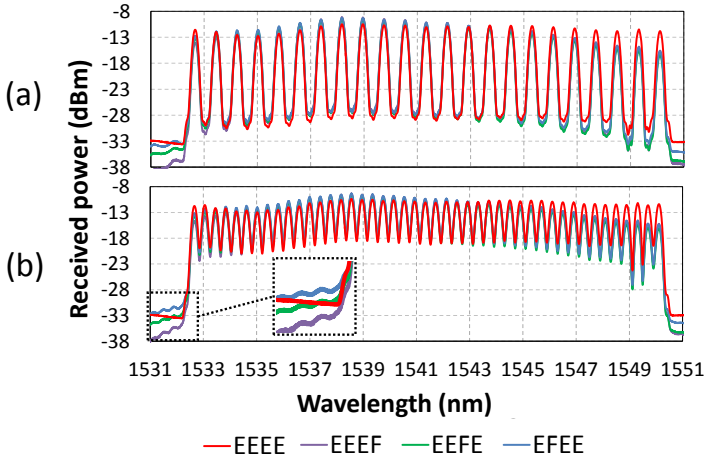

Fig. 2. Received spectra after 4x75km spans with transponder set at 193.5THz (1549.3nm) for (a) 100GHz channel spacing and (b) 50GHz channel spacing. RBW=0.02nm.

BER vs OSNR curves for $EEEE_{100/50}$ and $EEEF_{100/50}$ are presented in Fig. 3 at three representative f_{tsp} across the band. It should be emphasized that a direct comparison between the two amplifier chains cannot be made as the internal gains/losses/noise figures of the EDFA and FOPA were different. However, a comparison is useful to assess how close to 'EDFA-like' performance the HPL-FOPA can attain in its current form.

For both channel spacings, an OSNR penalty is observed for the FOPA-case which increases with frequency separation of the signal from the pump. This is consistent with previously reported results and is attributed primarily to the pump phase modulation used to counteract SBS in the FOPA HNLF. The phase modulation induces ~GHz gain fluctuations on the signals, thus effectively reducing SNR at the receiver. This has been shown to increase in severity away from the pump, and in particular for wavelengths beyond the gain peak [24-26]. This effect can be significantly reduced or removed by lowering the required level of pump phase modulation needed in the FOPA which can be accomplished by increasing the SBS threshold of the HNLF using an appropriate strain or temperature gradient [27], and will be the subject of further study. Another source of wavelength-dependent penalty is the magnified transfer of relative intensity

noise (RIN) from pump to signals [28]. This may be reduced using a lower RIN pump. At low OSNR, the EEEF performance converges close to EEEE for both channel spacings.

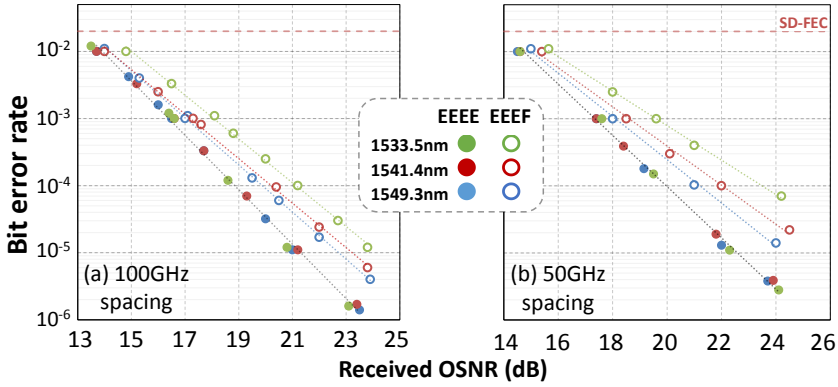

Fig. 3. BER vs received OSNR curves for three signals across the band with (a) 100GHz (b) 50GHz spacing

The comparative performance between 50GHz and 100GHz is explicitly examined in Fig. 4(a), where the BER performance is characterized for all signals across the band for the EEEE and EEEF sequences. The EEEE baseline performance at 50GHz is seen to be slightly degraded relative to $EEEE_{100}$, most likely due to increased noise at f_{tsp} arising from the DWDM emulation technique. It can be seen firstly that all signals are significantly below the SD-FEC threshold (~$1.5x10^{-2}$) and can thus be considered error free. In comparison with $EEEE_{50/100}$, a larger BER penalty is seen for $EEEF_{50}$ compared to $EEEF_{100}$. We believe this is due to the increased FWM crosstalk arising from the doubled channel count. Both $EEEF_{50}$ and $EEEF_{100}$ show the BER increasing with wavelength separation from the pump (λ_p=1564.4nm) which confirms the trend observed in Fig. 3. Example constellation diagrams are also shown for f_{tsp}=195.6THz (1532.68nm) in the $EEEE_{100}$ and $EEEF_{100}$ systems. It can be seen that the constellations show very similar circular distributions, but with slightly increased noise in the FOPA case.

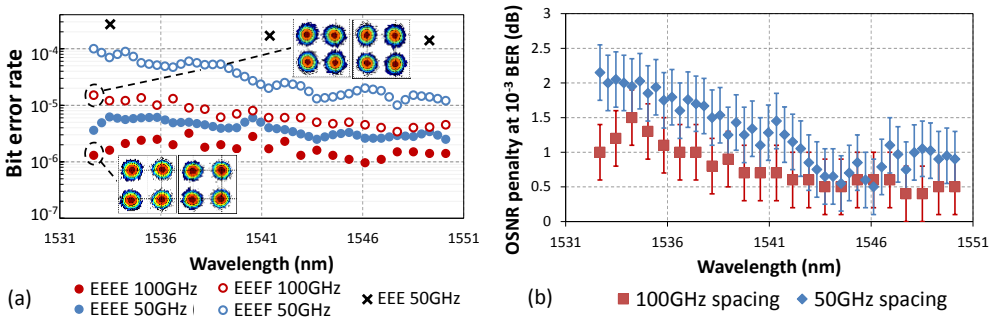

Fig. 4. (a) BER vs signal wavelength for EEEE and EEEF at 50GHz/100GHz channel spacing with no receiver noise added. Two example constellations are inset. Also displayed is EEE at 50GHz spacing, with a 150km span included between final two EDFAs. (b) OSNR penalty at 10^{-3} BER comparing $EEEE_{50/100}$ with $EEEF_{50/100}$

We have seen that the inclusion of the FOPA (EEEF) imparts a penalty over the use of four EDFAs (EEEE) in a 4x75km system. However, it is instructive to examine a system of the same overall length but with only three EDFAs (EEE) used, and compare the FOPA performance. Figure 4(a) plots three BER measurements across the band for an alternative 75km/75km/150km EEE system using 50GHz channel spacing. It can be seen that the BER is significantly degraded compared to the FOPA $EEEF_{50}$ system. This is attributed to a reduction in received OSNR of ~4dB observed on the received spectrum (not shown) arising from the

150km final span (loss of ~30dB). Thus, even with the BER penalty arising from the currently necessary use of pump phase modulation, the overall system performance *is benefitted by the inclusion of the FOPA due to improved system OSNR* compared with simply bypassing it. It should also be noted that the noise figure of the final EDFA reduced from ~11dB in the $EEEF_{50}$ case (75km spans) to ~5.5dB in the EEE_{50} case (150km final span) due to automatic tuning of an internal mid-stage VOA within the final EDFA from maximum to minimum loss in order to maintain flat-gain. If the noise figure had stayed constant, the benefit shown by the FOPA would have been larger.

Figure 4(b) summarizes the 4x75km EEEF OSNR penalty at 10^{-3} BER against wavelength for the two channel spacings in comparison with the EEEE system. As expected from the above results, a wavelength-dependent penalty is observed with a minimum/average/maximum penalty of 0.4/0.8/1.5 dB obtained at 100GHz-spacing, rising to 0.5/1.3/2.2 dB at 50GHz. Measurement error for these results is estimated to be ±0.5dB owing to multiple subtractions in the OSNR penalty calculation. As noted above, this penalty is not intrinsic to the FOPA gain process itself but arises due to a range of engineering and physical factors which are required to facilitate the gain process. As such, it should be possible to reduce the penalty as a result of future efforts.

3. Cascaded HPL-FOPA in recirculating loop arrangement

3.1 Experimental setup

To investigate cascaded HPL-FOPA amplification and transmission, the experimental set-up was rearranged to that of Fig. 5. The HPL FOPA was modified slightly to include an additional C/L splitter (loss ~0.8dB) at the output. This filter removed the L-band idlers to avoid them recirculating back into the FOPA. The FOPA net-gain was therefore reduced to ~15.2dB for the same pump conditions. The Oclaro transponder used in the previous in-line experiments was not able to receive a burst mode signal from a recirculating loop, and so an alternative Tx/Rx was employed. A 100kHz linewidth tunable laser provided the "channel under test" at frequency f_{sig}, and QPSK modulation applied to it using a standard I-Q nested Mach-Zehnder modulator. The electrical data patterns applied for QPSK were 30Gb/s normal and inverse 2^{31}-1 pseudo random binary sequences (PRBS) with a relative delay between the in-phase (I) and quadrature (Q) components of 300 symbols. A polarization multiplexing emulator (PolMux) with a relative delay of ~2ns between polarization states was then used to produce a 120Gb/s PDM-QPSK signal. As before, the signal was coupled with shaped broadband ASE to emulate different DWDM channel counts and channel spacing. An EDFA was used to set the DWDM launch power into the recirculating loop.

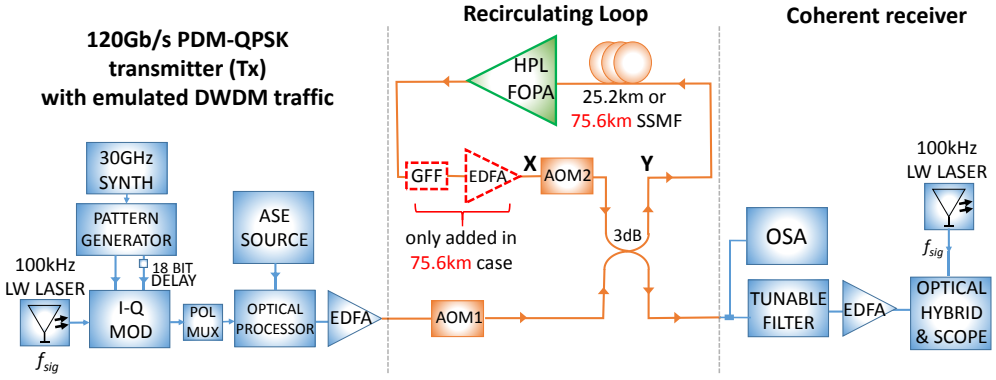

Fig. 5. Experimental set-up of DWDM HPL-FOPA recirculating loop transmission arrangement showing cascaded FOPA-only amplification using either 25.2km of SMF within the loop or (in red), 75.6km of SSMF together with a GFF and EDFA used to counter the loop switching losses. Abbreviations not referred to in the main body of the text are: LW=linewidth; MOD=modulator; Scope=real-time oscilloscope and offline DSP.

The loop consisted of a first acousto-optical modulator (AOM 1) for gating in data, followed by a 2x2 3dB coupler which defined the input and output of the loop as well as the recirculating region. Within the loop region itself, the signals first passed through a length of transmission fiber (see below), followed by the HPL-FOPA, and finally a second AOM 2 for gating data out of the loop. The combined passive loss of AOM 2 and the 3dB coupler (points X to Y in Fig. 5), and several patch-cord connectors was ~9dB. The transmission spans investigated were either:

a) 25.2km of Sterlite SSMF with insertion loss of 4.9dB. In this case, the FOPA compensated for the 9dB loop switching losses *and* the transmission fiber.

b) 75.6km of Sterlite SSMF with loss of 15.2dB. In this case, an adjustable gain flattening filter (GFF) was used within the recirculating loop, together with an EDFA to compensate for the combined GFF and loop switching losses (~13dB in total). The HPL-FOPA compensated for the 75.6km transmission fiber only. The EDFA was not ideally optimized for 13dB gain, and was operating with high noise figure as a result (>11 dB). However, this was deemed acceptable due to its position after the FOPA and was not found to be a limiting factor of the overall system performance.

Table 1. Channel plan information for HPL-FOPA recirculating loop

Channel Count	Channel spacing (GHz)	Start frequency /THz (wavelength /nm)	End frequency /THz (wavelength /nm)
10	100	194.2 (1543.7)	195.1 (1536.6)
20	50	194.15 (1544.1)	195.1 (1536.6)
30	50	193.9 (1546.1)	195.35 (1534.7)

Three different DWDM channel plans were analyzed: 10, 20 and 30 channels using either 100GHz or 50GHz spacing. Their relative position within the spectrum was chosen to be at the flattest part of the HPL-FOPA gain spectrum in order that gain-flattening was not essential. Specific details are given in Table 1. It should be noted that it was not possible to employ the full 2.3THz bandwidth demonstrated in Section 2 within the recirculating loop. This was due to a combination of the FOPA gain roll off at the extreme wavelengths and the amount of loop switching loss together with some practical resource issues such as the granularity of available transmission fiber spans. Ideally, slightly shorter spans would have allowed a wider bandwidth to be demonstrated, but they were not available to us. Similarly, increasing the FOPA gain further using higher pump powers would certainly have offered increased bandwidth but at the expense of increased penalty and a lower maximum number of recirculations [14].

The Rx was a standard polarization-diverse coherent receiver with analogue to digital conversion achieved using an 80GSa/s, 36GHz bandwidth real-time oscilloscope. Digital signal processing (DSP) was performed offline using standard algorithms for signal recovery and linear transmission impairment compensation. Data pattern were typically ~240kbit in length with bit-wise error counting performed on the recovered pattern. Q^2 factors were then either estimated from the derived constellation for BER $<10^{-3}$ or converted from the actual BER for $>10^{-3}$ [29].

3.2 25.2km transmission fiber recirculation results using FOPA-only amplification

Figure 6 summarizes the cascaded performance of the HPL-FOPA at 50GHz and 100GHz spacing when used as the only amplifier within the recirculating loop, whilst transmitting over the 25.2km SSMF span. We believe this is the first time this has been achieved. No levelling of signals was employed due to the restricted gain budget available. Error bars are estimated at ±0.5dB after averaging numerous measurements at fixed operating points to ascertain the spread of received Q^2 values. For visual simplicity, we define a Q^2 of 7dB (~1.5×10^{-2} BER)

which is close to the SD-FEC limit as the maximum performance metric of the cascaded system (indicated as dashed red line in the plots).

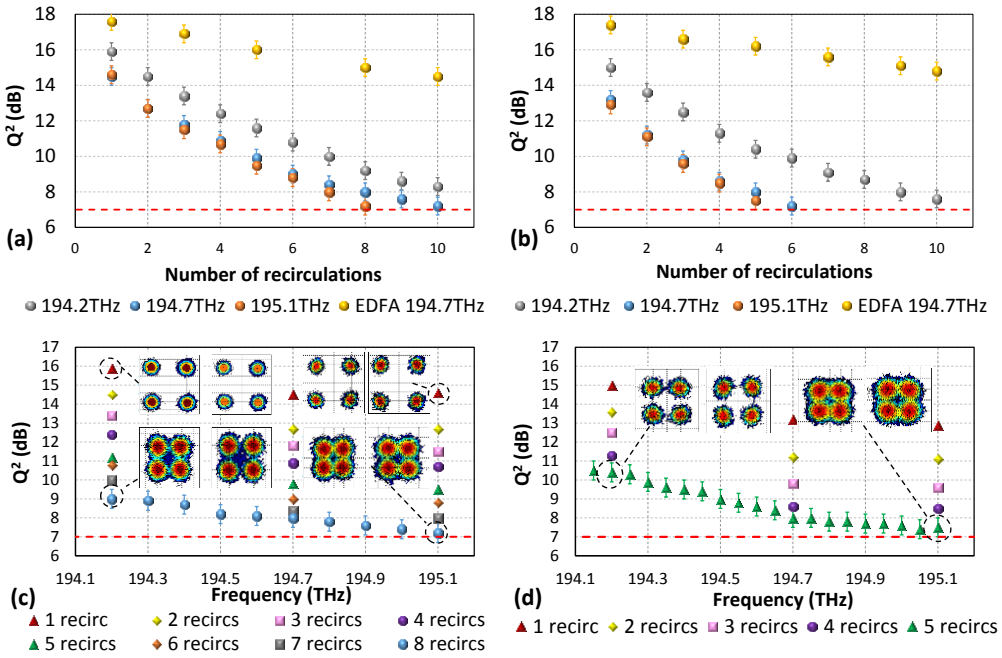

Fig. 6. Q^2 against number of recirculations for independent HPL-FOPA and EDFA amplification with 25km of transmission fiber per recirculation for (a) 10x100GHz-spaced signals and (b) 20x50GHz-spaced signals. (c) Q^2 against frequency for different numbers of recirculations, with 10x100GHz-spaced signals and (d) 20x50GHz-spaced signals. Example constellation diagrams are shown in inset for various operating points.

The evolution of performance with number of recirculations is shown in Fig. 6(a) and 6(b) for the 10x100GHz and 20x50GHz channel plans respectively. In both cases, the Q^2 of three representative signals spanning the transmission band are shown, together with the equivalent performance when a standard laboratory EDFA (same as Section 2) was swapped as a direct replacement for the FOPA. It can be seen that in the FOPA-only case, the performance for each signal is degraded in comparison with the EDFA, with the differential growing as the number of recirculations increases. As will be seen below, this is not due to significant differences in OSNR degradation (noise figure) but is, we believe, primarily due to the signals picking up additional noise from the dither and RIN of the pump as described in Section 2.1. A similar trend to the in-line system is also seen for the maximum number of cascades for both signal spectra densities as f_{sig} is increased. In Fig. 6(a) with 100GHz-spacing, the lowest frequency (longest wavelength) signal at 194.2THz shows ~1dBQ^2 margin after ten recirculations (total transmission distance of 252km), but for higher f_{sig} (shorter wavelength) the signal quality reduces. The signal at 195.1THz only achieves eight recirculations or 201.6km transmission. For a comparison of the effect of different signal spectral density, Fig. 6(a) and 6(b) can be compared directly, bearing in mind that the channel count and thus total signal power is double in the twenty channel (50GHz) case. Here the observations are interesting: for f_{sig} =194.2THz, performance for twenty channels tracks the ten channel case quite closely (albeit with slightly lower Q^2 at each point), achieving ten recirculations in total. However as f_{sig} is increased from 194.7THz to 195.1THz, the maximum number of recirculations drops to six and five respectively. This is considerably worse performance than in the ten channel case, and is attributed to increased WDM crosstalk.

At the maximum number of recirculations (eight for 100GHz spacing, five for 50GHz spacing), the Q^2 for each transmitted signal is plotted, and some example recovered constellation diagrams are also included to show the range of noise variation seen across the band. It is clear that for the twenty channel case (50GHz spacing), the Q^2 differential across the band (ΔQ^2) is considerably larger (3dB) than the ten channel case (1.8dB) even after five recirculations.

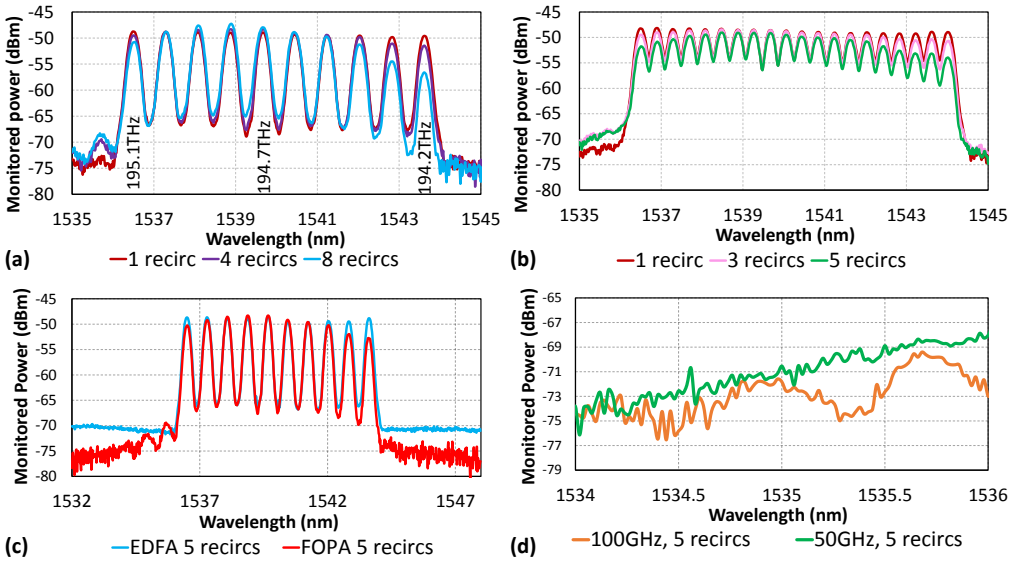

Fig. 7. Optical spectra at output of the 25.2km (non-GFF) recirculating loop incorporating the HPL-FOPA for (a) 10x100GHz-spaced signals at 1, 4 and 8 recirculations and (b) 20x50GHz-spaced signals at 1, 3 and 5 recirculations. (c) Comparison of EDFA-only and FOPA-only spectra after five recirculations (d) Comparison of FOPA-only crosstalk level at 5 recirculations for 50GHz spacing (green) and 100GHz spacing (orange).

To help clarify the different performance seen for the different channel spacings, optical spectra for both the 10x100GHz and 20x50GHz-spaced signals in the FOPA-only case are shown in Fig. 7 for different numbers of recirculations. The resolution bandwidth of the optical spectrum analyzer (OSA) was 0.1nm (12.5GHz). As mentioned previously, no levelling of the spectra was employed, and so these spectra represent the cumulative spectral shape obtained from repeated amplifications. The evolution of the OSNR is clearly seen, with the signals at the extreme of the band showing reduction in peak power as the recirculations increase for both 50GHz and 100GHz spacing. In fact, for the best-performing signal at f_{sig}=194.2THz, the OSNR is actually *worse* than neighboring signals having relatively poorer transmission performance (e.g. 194.7THz or 195.1THz). This confirms that the OSNR is not the limiting factor for this FOPA, and the penalty actually arises predominantly from the other mechanisms discussed previously which are not visible on an optical spectrum. This conclusion is verified again in Fig. 7c, where the EDFA and FOPA spectra are compared directly after five recirculations. It can be seen that the noise floor for the FOPA is actually lower than that of the EDFA in some parts of the spectrum, indicating a lower optical noise figure. However, the presence of four-wave mixing crosstalk is seen to the low wavelength (high frequency) side of the spectrum (~20dB below peak) which degrades the effective OSNR for these channels, and partially explains the reduced performance here. Figure 7(d) shows this region in more detail in the 10 channel (100GHz spacing) and 20 channel (50GHz spacing) cases. Due to the limited resolution bandwidth of the OSA (0.1nm), the channelized nature of the crosstalk is not observable in the

20 channel case, but it is clear that the crosstalk is higher than for the ten channels as suggested. This again helps explain the reduced performance seen for the 20 channels.

3.3 75.6km transmission fiber recirculation results using FOPA, GFF and EDFA

As detailed in Section 3.1, the recirculating loop was next reconfigured to comprise a 75.6km SSMF transmission span and a gain flattening filter (GFF). The loss of this longer span was 15.2dB, while the GFF loss was ~4dB with any levelling losses added to this. The GFF allowed wavelength dependent losses to be set with 0.25nm resolution, and was adjusted to level the spectrum after ten recirculations. The FOPA average gain of 15.2dB therefore compensated completely for the span loss of central signals, but outer signals received slightly less due to the gain roll-off. The loop passive losses remained unchanged at ~9dB, and therefore an additional EDFA with gain of 13dB was also required inside the loop to compensate for this and GFF loss. Spectra for 1, 4 and 8 recirculations are shown for the 10x100GHz and 20x50GHz cases in Fig. 8(a) and 8(b) respectively, showing significantly flatter signal profiles than the unlevelled previous case as would be expected, together with blocked out-of-band crosstalk.

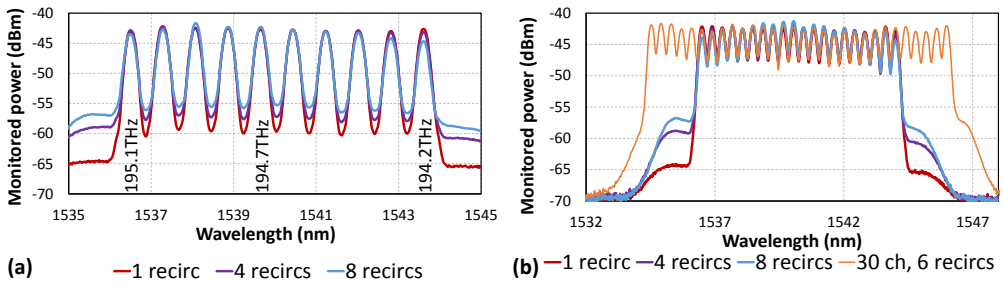

Fig. 8. Optical spectra at output of the 75km recirculating loop incorporating the HPL-FOPA with GFF and EDFA for (a) 10x100GHz-spaced signals at 1, 4 and 8 recirculations and (b) 20x50GHz-spaced signals at 1, 4 and 8 recirculations, and 30x50GHz-spaced signals at 6 recirculations.

Figure 8(b) also highlights the record achievement of wider bandwidth operation after transmitting 30x50GHz signals (193.9-195.35THz) for six recirculations (453.6km). Wider bandwidth in this way was possible because the GFF and EDFA combination effectively allowed a bespoke power versus distance profile to be optimized for each transmitted signal within the loop, whilst also preventing out-of-band ASE build-up and growth of signal power variations. Nonetheless, OSNR for the same number of recirculations is reduced from Fig. 7 as would be expected due to the higher overall losses experienced by the signals.

Figures 9(a) and 9(b) show the trend of Q^2 against number of recirculations for the 20x50GHz and the 30x50GHz cases respectively for three signals across the band. It can be seen that the maximum number of recirculations decreased from eight (604.8km transmission) to six (453.6km) after expanding the bandwidth from 1THz (20x50GHz) to 1.5THz (30x50GHz). This reduction continues the trend of reduced signal quality with frequency for a now higher maximum transmitted f_{sig} of 195.35THz. However for lower f_{sig} the performance for 30 signals is seen to be at least as good as the 20 signal case which on the surface is surprising as nonlinear crosstalk might be expected to be higher. However due to the more rapid FOPA gain roll off in the low frequency region for 30 channels compared with 20, it is likely that increased supplementary gain was obtained from the EDFA to maintain flatness. The proportional penalty from the FOPA was therefore likely lower. It can be seen that the interplay between the spectral profiles of the GFF levelling loss, FOPA gain and EDFA gain within the recirculating loop is complex and hence difficult to ascertain the exact proportions of gain contributions from each amplifier, especially as the GFF was adjusted differently for each channel count in order to flatten the received spectrum.

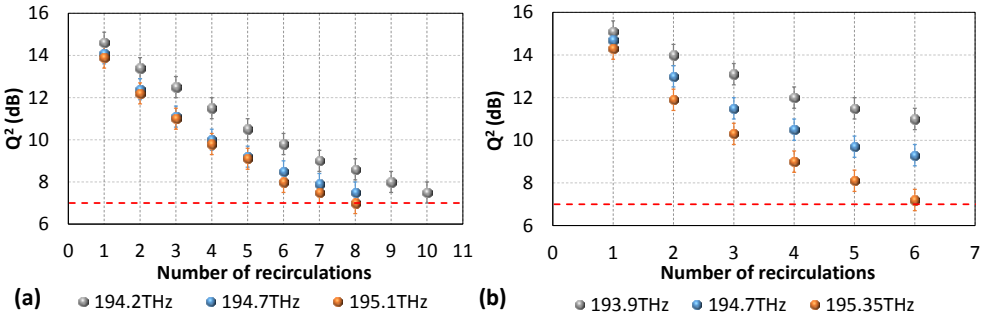

Fig. 9. Q^2 against number of recirculations for 75.6km of transmission fiber per recirculation, and the loop incorporating the HPL-FOPA, a gain-flattening filter and an EDFA for (a) 20x50GHz-spaced signals and (b) 30x50GHz-spaced signals.

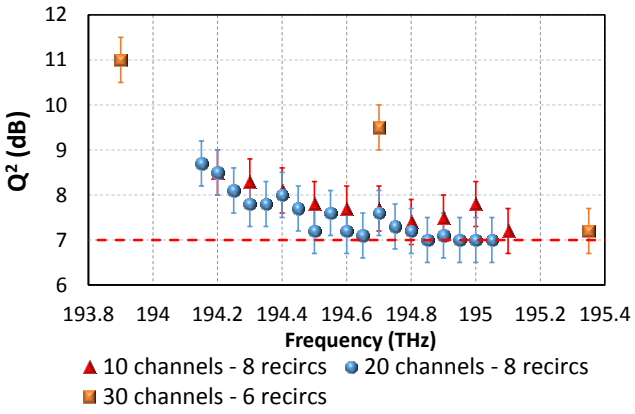

Fig. 10. Q^2 against frequency for 10x100GHz signals (red triangles) and 20x50GHz signals (blue circles) after 8x75.6km recirculations. Three representative f_{sig} are shown for 30x50GHz-spaced signals (yellow squares) after 6x75.6km recirculations.

Figure 10 shows the full transmission band performance after eight recirculations (604.8km total transmission) for 10x100GHz and 20x50GHz signals, and six recirculations (453.6km) for 30x50GHz signals (three representative signals were measured). The disparity between the 100GHz and 50GHz spacing is much smaller than in the 25km FOPA-only non-levelled loop, with the 50GHz-spaced signals achieving a maximum of eight recirculations here rather than five previously. There is no obvious reason for this improvement and possibly indicates the impact of measurement uncertainty seen for Q^2, coupled with the level of penalty granularity induced from each recirculation. This suggests that further optimization of the described systems should be possible, but this may not significantly extend transmission reach unless the influence of the key penalty factors described earlier are reduced in magnitude (e.g. pump phase modulation). For improved performance over the whole band, it might also be suggested that the entire set of signals should be shifted to lower frequencies as performance appears to be superior here (especially in the 30 channel case of Fig. 10). However, this is somewhat illusory due to the underlying gain roll-off seen by the FOPA in this region. Translating the signals would therefore only be possible whilst receiving the supplementary gain from the EDFA, and would not be possible with this FOPA operating in isolation. However, we believe much wider bandwidths are certainly possible using the HPL-FOPA architecture, and this will be a key driver for our future work.

Conclusions

For the first time we have demonstrated DWDM transmission in optical systems incorporating a PI-FOPA to compensate for fiber span loss. The PI-FOPA employed a diversity-loop HPL architecture to obtain a practical level of net-gain (16dB) and gain bandwidth of 2.3THz (~18nm). As part of a representative 4x75km in-line system, 45 x 50GHz-spaced signals were transmitted ('equivalent' data-rate of 4.5Tb/s). The OSNR penalty at a BER of 10^{-3} was only 0.8dB at 100GHz spacing and 1.3dB at 50GHz spacing (averaged over all signals). The PI-FOPA was also incorporated in two recirculating loop experiments. In the first, we accomplished PI-FOPA-only cascaded amplification for the first time using a 25.2km length of SSMF (~5dB) within the recirculating loop. No additional amplification was required here as the PI-FOPA had sufficient net-gain to compensate for the loss of the transmission SSMF and the loop switches and passive components (~9dB). Maximum achieved numbers of recirculations for all signals were: eight for 10x100GHz-spaced signals and five recirculations for 20x50GHx-spaced signals. In the second recirculating loop, the transmission span was extended to 75.6km (~15.2dB loss), which was compensated for by the PI-FOPA. A GFF was also included, with a supplementary EDFA supplying gain to compensate for the GFF loss and that of the loop switches and passives. Eight recirculations for all 20x50GHz signals were achieved resulting in a record total transmission distance of 604.8km. We consider this progress to be a key stepping-stone towards realizing a practical in-line FOPA with bandwidths and performance exceeding traditional EDFAs.

Funding

UK Engineering and Physical Sciences Research Council (EPSRC) grants EP/M005283/1 (UPON) and EP/J017582/1 (UNLOC); II-VI for CASE studentship of V. Gordienko.

Acknowledgments

Oclaro are thanked for the loan of the transponder used in the in-line experiments. Sterlite are thanked for the loan of the transmission fibre spans. The data reported in this paper is available at http://doi.org/10.17036/researchdata.aston.ac.uk.00000256 as part of the UK EPSRC open access policy.